

1. Introduction

In order to investigate the structure of the primary donor P⁺-860 in bacterial photosynthesis, electron-spin double and triple magnetic resonance techniques have been used, yielding information about the hyperfine interactions [1–5]. Another method to obtain information about, in particular, the weak electron–nuclear couplings of this radical, is frequency analysis of the electron spin echo envelope modulation (ESEEM) [6,7]. These couplings, e.g. of the nitrogens, may provide critical data with respect to the special pair model for P⁺-860 [1–5] as compared to a monomer model in which the two lowest molecular orbitals of the cation are mixed [8].

In modulation studies [9–12] carried out on the chlorophyll a cation radical *in vitro* and on the oxidized primary donor of spinach chloroplasts the ESEEM appeared to be dominated by the nuclear quadrupole couplings of the ¹⁴N nuclei. From these

frequencies the isotropic hyperfine constants of the ¹⁴N nuclei were estimated.

A different approach to obtain information about the hyperfine couplings is isotopic substitution of ¹⁴N by ¹⁵N. Because of the absence of a quadrupole moment in ¹⁵N nuclei ($I = \frac{1}{2}$), echo modulation effects are only due to hyperfine interactions. Hence a frequency analysis of the ¹⁵N substituted P⁺-860 modulation patterns yields the hyperfine constants directly.

In this report we present a comparison of the echo modulation frequencies in ¹⁴N, and in ¹⁵N substituted P⁺-860 of the photosynthetic purple bacteria *Rhodospirillum rubrum* and *Rhodospseudomonas sphaeroides*.

2. Experimental

The ESE experiments were performed on an X-band ESE spectrometer similar to that described in

ref. [13]. ESEEM patterns were recorded using the two-pulse echo and the stimulated echo (SE) technique. In the former technique, the echo intensity is recorded as a function of the time τ_{12} between the first and second microwave pulse, in the latter τ_{12} is fixed while the SE intensity is recorded as a function of the time τ_{23} between the second and third microwave pulse. The frequency analysis of the modulation patterns was carried out using a program [14] based on the maximum entropy method (MEM).

Chromatophores of the purple bacteria *Rhodospirillum rubrum*, grown as in ref. [15], were prepared by sonication of the cells and centrifugation for 30 min at 13000 rpm yielding the chromatophores in the supernatant. ^{15}N enriched cells of *Rhodospseudomonas sphaeroides* were grown in Hutner's medium [16] containing ^{15}N ammonium sulfate as the sole nitrogen source and yeast concentrate (Sigma, Munich) instead of yeast extract. The enrichment of the chlorophylls was determined by mass spectroscopy of the bacteriomethylpheophorbide a to 85%. Reaction centers were prepared by a modification of the method of Jolchine and Reis-Husson [17] using two subsequent solubilization steps with 0.25% LDAO. The oxidation of P-860 was accomplished by illuminating the samples during freezing to 77 K.

3. Results

Isotopic substitution of ^{14}N by ^{15}N results in a significant change in the two-pulse echo envelope modulation pattern of the primary donor P^+-860 (figs. 1A, 1B). A frequency analysis of these modulation patterns is presented in fig. 2. This analysis yields two frequencies (0.9 and 2.6 MHz) for the ^{14}N chromatophores, and one (2.7 MHz) for the ^{15}N material.

The application of the two-pulse echo sequence to obtain information about the modulation frequencies has two major disadvantages: (1) the two-pulse echo decay time is determined by the phase-memory time which in our case means that the recording of the two-pulse echo decay trace is limited to a maximum τ_{12} value of about 2.5 μs . (2) A frequency analysis of a two-pulse echo decay may in addition to the nuclear transition frequencies also yield their sum and difference frequencies.

In order to circumvent these two serious limita-

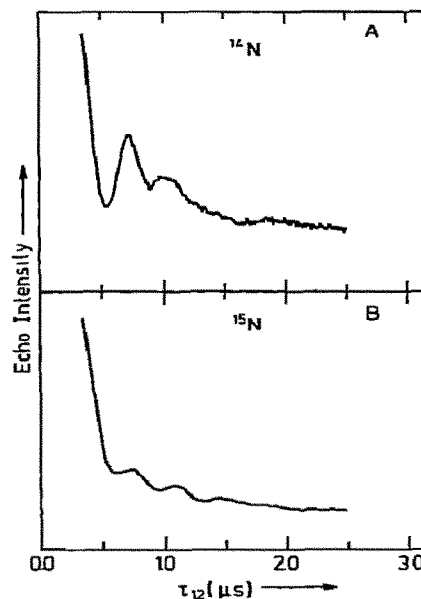


Fig. 1. Two-pulse echo envelope modulation traces of (a) ^{14}N P⁺-860 and (b) ^{15}N substituted P⁺-860. Temperature 4 K, microwave pulse power 20 W, duration of π pulse 120 ns.

tions we carried out stimulated echo experiments. The stimulated echo decay is only determined by the spin-lattice relaxation which is usually much longer than the phase-memory time. Therefore, the stimulated echo decay can be recorded during a longer time interval, thus reducing the linewidth in the corresponding frequency domain. Another advantage of the SE

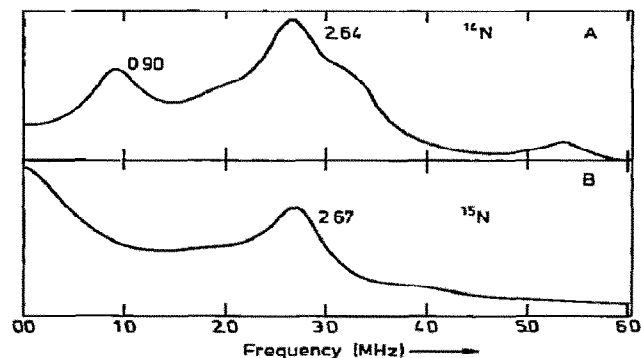


Fig. 2. Frequency spectra obtained by the MEM corresponding to the two-pulse echo modulation traces of fig. 1. (a) ^{14}N P⁺-860, (b) ^{15}N P⁺-860.

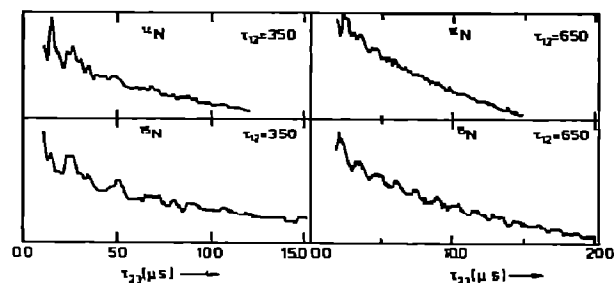


Fig. 3. Some characteristic stimulated echo modulation traces. The fixed time τ_{12} (in ns) are indicated. Conditions as in fig. 1

method is that the decay is modulated by nuclear transition frequencies without their sums or differences (at least when one nucleus is considered).

For both the ^{14}N and ^{15}N samples the SE decay was recorded at several τ_{12} to avoid missing modulation frequencies due to possible suppression effects [6]. Some of these traces are shown in fig. 3. The corresponding frequency spectra are depicted in figs. 4A, 4B. From each figure four frequencies are extracted which are assumed to be real modulation frequencies, because their intensity is high and/or they appear in the frequency spectra at several τ_{12} . Other, low-intensity peaks in the frequency spectrum that occur at only one τ_{12} are disregarded. The averaged modulation frequencies are given in tables 1 and 2.

Comparing tables 1 and 2 with the frequencies of figs. 2A, 2B it is seen that the frequencies found by the analysis of the two-pulse echo modulation envelope are confirmed. Moreover, the stimulated echo modulation analysis yields some additional frequencies.

Table 1
Stimulated echo modulation frequencies of ^{14}N P⁺-860

^{14}N line	Frequency a) (MHz)	Quadrupole set b)
1	0.5	(a)
2	0.9	(a), (b)
3	1.6	(a), (b)
4	2.5	(b)

a) Error ± 0.1 MHz.

b) The quadrupole frequencies ν_0, ν_{\pm} are given by $\nu_0 = 2K\eta$ and $\nu_{\pm} = K(3 \pm \eta)$, where $K = a^2 qQ/4h$ and η is the asymmetry parameter [18].

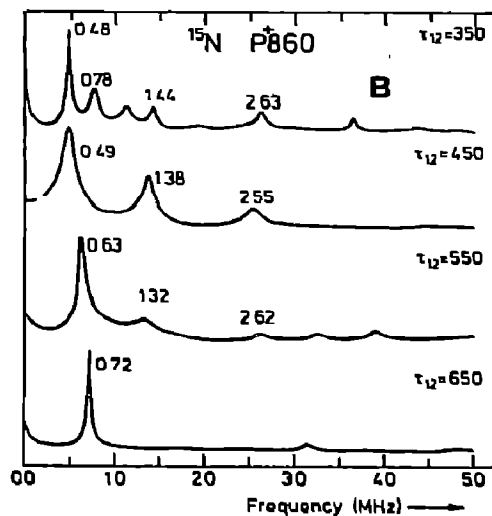
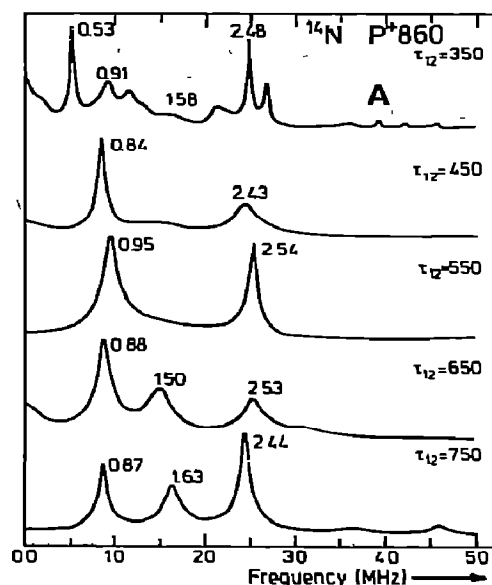


Fig. 4. The total set of MEM frequency spectra obtained for (a) ^{14}N P⁺-860, (b) ^{15}N P⁺-860. The values of the main frequencies are indicated.

4. Discussion

As we are performing our experiments on frozen, i.e. immobilized, disordered systems the nuclear quadrupole interactions are not averaged out by motional

Table 2
Stimulated echo modulation frequencies of $^{15}\text{N P}^+\text{-860}$

Line	Modulation frequency ^{a)} (MHz)	A_{\perp} ^{b)}	A_{iso} (calc.) ^{c)}	A_{\parallel} (calc.) ^{d)}	ENDOR results [5]		
					A_{\perp}	A_{iso}	A_{\parallel}
1	0.49	1.86	2.1	2.7	1.9	2.22	2.9
2	0.71	1.42	1.6	2.0		1.61	
3	1.38	0.08	0.1	0.1			
4	2.60	2.36	2.7	3.4	2.3	2.60	3.1
						1.05	

^{a)} Error ± 0.08 MHz ^{b)} From $\nu_{\text{mod}} = \nu_Z \pm \frac{1}{2}A$ where the ^{15}N nuclear Zeeman frequency $\nu_Z = 1.42$ MHz. Error ± 0.16 MHz.
^{c)} $A_{\text{iso}} = \frac{1}{3}(2 + R)A_{\perp}$ with $R = A_{\parallel}/A_{\perp} = 1.44$ as reported in ref. [5]. ^{d)} $A_{\parallel} = RA_{\perp}$.

narrowing. Dikanov et al. [11] pointed out that in randomly oriented samples the ^{14}N quadrupole frequencies can be modulation frequencies when the quadrupole splitting is larger than the hyperfine splitting.

We follow a similar procedure to interpret the ^{14}N modulation frequencies as listed in table 1. Analogous to the results obtained for the primary donor in spinach and for Chl a^+ in vitro [11] the modulation frequencies are assumed to be nuclear quadrupole frequencies and within the experimental error (± 0.08 MHz) two different sets can be assigned. For the set consisting of 0.5, 0.9 and 1.6 MHz (a) as well as for the set 0.9, 1.6 and 2.5 MHz, (b) the sum of the first two frequencies equals the third frequency. This property is characteristic for nuclear quadrupole frequencies, belonging to one nucleus. That two sets of quadrupole frequencies are observed can be explained by the fact that there are two different electron configurations for the electrons surrounding the nitrogen nuclei [11].

Following [11] the range of the isotropic hyperfine constant (A_{iso}) of the ^{14}N nuclei is estimated to be $1.2 < A_{\text{iso(a)}} < 2.9$ MHz ($K = 0.42$ MHz with $\eta = 0.68$) and $0.7 < A_{\text{iso(b)}} < 3.4$ MHz ($K = 0.68$ MHz with $\eta = 0.66$). Here K is the quadrupole constant divided by four and η the asymmetry parameter [11]. For the ^{15}N nuclei this yields $1.7 < A_{\text{iso(a)}} < 4.1$ MHz and $1.0 < A_{\text{iso(b)}} < 4.8$ MHz. These ranges are in good agreement with the ENDOR results for $\text{P}^+\text{-860}$ of *Rhodospseudomonas sphaeroides* R-26 published recently by Lubitz [5].

In the ^{15}N substituted reaction centers the quadrupole moment is absent, therefore the SE modulation must be due to the hyperfine and nuclear Zeeman

interactions. The averaged transition frequencies obtained from fig. 4B are listed in table 2.

Before comparing our ^{15}N modulation frequencies with the ENDOR results of [5] we have to consider the following: (1) The hyperfine constants of nitrogen nuclei are in general anisotropic with approximate axial symmetry. (2) Our samples are frozen solutions and thus immobilized and randomly oriented. Comparison of the echo results as listed in table 2 and those of Lubitz et al. (also listed in table 2) show that the hyperfine coupling constants 1.86 ± 0.16 MHz and 2.36 ± 0.16 MHz, obtained from the SE modulation frequencies 0.49 MHz (line 1) and 2.60 MHz (line 4) respectively, are in good agreement with the two values for A_{\perp} found by Lubitz et al. [5]. This is a rather unexpected result, as theoretically the modulation depth is proportional to $\sin^2\theta \cos^2\theta$, where θ is the angle of the magnetic field with respect to the axis of the axially symmetric hyperfine tensor [6,7]. Multiplied by the distribution function for an axially symmetric system in a randomly oriented sample ($\propto \sin\theta$) this gives a maximum modulation depth at $\theta = 51^\circ$. The corresponding effective hyperfine coupling is close to A_{iso} , not to A_{\perp} . Note that the prevalence of frequencies close to A_{\perp} cannot be due to incomplete excitation of all couplings by the amplitude of the microwave field, as in our analysis hyperfine couplings of magnitude larger than the difference between A_{\parallel} and A_{\perp} for any particular coupling are clearly visible. Unfortunately, there is little known about the modulation pattern in randomly oriented systems where $|A_{\parallel} - A_{\perp}|$ is of similar magnitude as A_{iso} . It will be necessary to carry out numerical calculations of the echo envelope modulation pattern for such systems to provide a theoretical basis for the

close correspondence between the hyperfine couplings obtained from frequency analysis of the echo modulation pattern and the perpendicular component of the hyperfine tensor.

If we accept that the ESEEM frequency analysis for our particular case yields frequencies close to A_{\perp} , then the line at 0.71 ± 0.08 MHz corresponds to the A_{\perp} value for the third ^{15}N hyperfine tensor, which is then 1.42 MHz. Note that from ESEEM measurements it is not possible to determine the sign of the hyperfine constants (they are positive [5]).

The remaining resonance in table 2 is almost equal to the nuclear Zeeman frequency (1.42 MHz) of the ^{15}N nuclei. It is either due to so-called "matrix ENDOR", i.e. couplings with the ^{15}N nuclei within the reaction center protein, or it represents the fourth nitrogen of $\text{P}^{+}\text{-860}$, which then must have a very small hyperfine coupling (0.08 ± 0.16 MHz).

As an additional check on the A_{\perp} values obtained, we calculated (table 2) the corresponding isotropic hyperfine constants (A_{iso}) and the parallel components (A_{\parallel}) of the hyperfine tensors. In this calculation we assumed that the anisotropy (defined as the ratio of A_{\parallel} and A_{\perp}) has an average value of 1.44 [5] and is equal for all four nitrogens. It is seen from table 2 that for lines 1, 2 and 4 the A_{iso} , and for lines 1 and 4 the A_{\parallel} , are in good agreement with those reported by Lubitz et al. [5]. Only the resonance at 1.38 MHz (line 3) does not agree with the reported ENDOR values, providing an agreement for its attribution to the ^{15}N nuclei of the matrix.

Irrespective of the individual assignments, the ^{15}N couplings of $\text{P}^{+}\text{-860}$ are on the average only half as large as the ones of BChl^{+} in solution. This reduction is in agreement with the special pair model for $\text{P}^{+}\text{-860}$ [1-5] rather than with a protein-induced mixing of the ground and excited state orbitals in a monomeric species [8].

In conclusion we wish to emphasize that the present study is the first in which the ESEEM frequencies of a disordered system with several inequivalent nuclei possessing a strongly anisotropic near-axial hyperfine tensor could be compared with ENDOR data. The finding that, contrary to the results for systems with weakly anisotropic hyperfine tensors [6, 7, 10], the ESEEM frequencies reflect the perpendicular component of the axial tensor, rather than the isotropic hyperfine coupling, calls for more extensive theoretical analysis.

Acknowledgement

We thank Lenneke Nan for preparing the chromatophores of *Rhodospirillum rubrum* and Dr. W. Schäfer (Martinsried, West Germany) for recording the mass spectra of the ^{15}N enriched sample. We thank Dr. J. Schmidt of the Center for the Study of the Excited State of Molecules for critically reading the manuscript. This work was supported by the Netherlands Foundation for Chemical Research (SON) with financial aid from the Netherlands Organization for the Advancement of Pure Research (ZWO).

References

- [1] A.J. Hoff and K. Möbius, Proc. Natl. Acad. Sci. US 75 (1978) 2296.
- [2] J.R. Norris, H. Scheer and J.J. Katz, in: The porphyrins, Vol. 4, ed. D. Dolphin (Academic Press, New York, 1978) ch. 3.
- [3] F. Lendzian, W. Lubitz, H. Scheer, C. Bubenzer and K. Möbius, J. Am. Chem. Soc. 103 (1981) 4635.
- [4] W. Lubitz, H. Lendzian, H. Scheer, J. Gottstein, M. Plato and K. Möbius, Proc. Natl. Acad. Sci. US 81 (1984) 1401.
- [5] W. Lubitz, R.A. Isaacson, E.C. Abresch and G. Feher, Proc. Natl. Acad. Sci. US, to be published.
- [6] W.B. Mims and J. Peisach, in: Biological magnetic resonance, Vol. 3 (Plenum Press, New York, 1981) ch. 5.
- [7] L. Kevan, in: Time domain electron spin resonance, eds. L. Kevan and R.N. Schwartz (Wiley, New York, 1979) pp. 279-339.
- [8] P.J. O'Malley and G.T. Babcock, Proc. Natl. Acad. Sci. US 81 (1984) 1098.
- [9] M.K. Bowman, J.R. Norris, M.C. Thurnauer and J. Warden, Chem. Phys. Letters 55 (1978) 570.
- [10] S.A. Dikanov, Y.D. Tsvetkov, M.K. Bowman and A.V. Astashkin, Chem. Phys. Letters 90 (1982) 149.
- [11] S.A. Dikanov, A.V. Astashkin and Y.D. Tsvetkov, Chem. Phys. Letters 101 (1983) 206.
- [12] M.C. Thurnauer and C.O. Clark, Photochem. Photobiol. 40 (1984) 381.
- [13] P. Gast, R.A. Mushin and A.J. Hoff, J. Phys. Chem. 86 (1982) 2886.
- [14] D. van Ormondt and K. Nederveen, Chem. Phys. Letters 82 (1981) 443.
- [15] H. de Klerk, R.G. Bartsch and M.D. Kamen, Biochem. Biophys. Acta 97 (1965) 275.
- [16] G. Cohen-Bazire, W.R. Sistrom and J. Stanier, J. Cell. Comp. Physiol. 49 (1957) 25.
- [17] G. Jolchine and F. Reis, Husson, FEBS Letters 40 (1974) 5.
- [18] A. Abragam, Principles of nuclear magnetism (Oxford Univ. Press, Oxford, 1961).